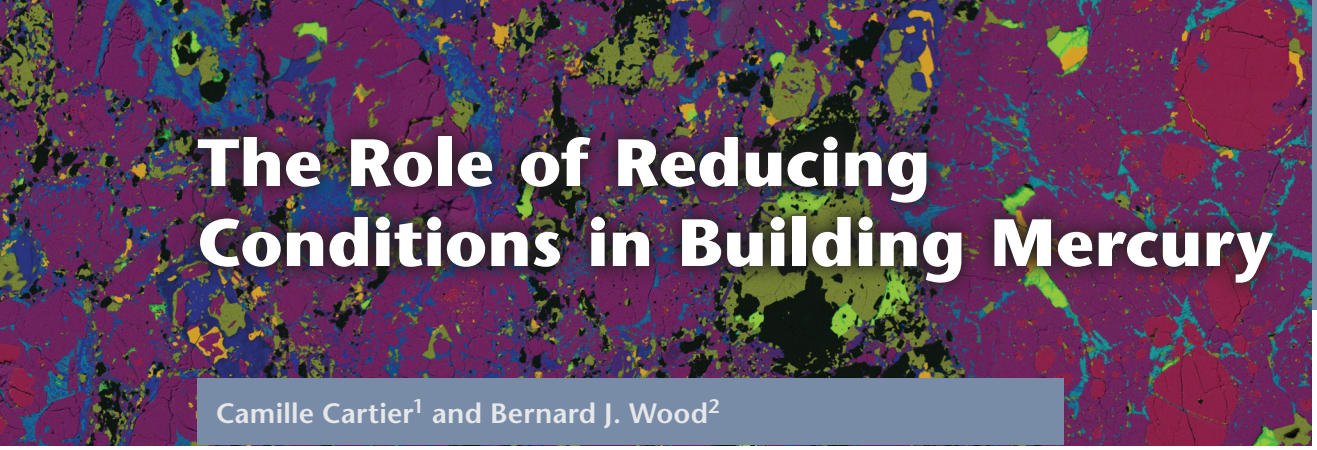

The Role of Reducing Conditions in Building Mercury

Camille Cartier[1] and Bernard J. Wood[2]

1811-5209/19/0015-0039$2.50 DOI: 10.2138/gselements.15.1.39

Extremely reducing conditions, such as those that prevailed during the accretion and differentiation of Mercury, change the "normal" pattern of behaviour of many chemical elements. Lithophile elements can become chalcophile, siderophile elements can become lithophile, and volatile elements can become refractory. In this context, unexpected elements, such as Si, are extracted to the core, while others (S, C) concentrate in the silicate portion of the planet, eventually leading to an exotic surface mineralogy. In this article, experimental, theoretical and cosmochemical arguments are applied to the understanding of how reducing conditions influenced Mercury, from the nature of its building blocks to the dynamics of its volcanism.

KEYWORDS: Mercury, enstatite meteorites, planetary differentiation, oxygen fugacity, element partitioning

INTRODUCTION

The bulk chemical composition of a planet is controlled by the nature of the primitive materials which accrete to it and by late accretionary processes such as giant impacts. The differentiation and structure of the resultant planet then develops through extensive melting to produce the "magma ocean" stage, which in turn leads to the formation of the core, the mantle and the primordial crust. During this stage, several phases are in equilibrium: a silicate liquid, a metallic liquid, and, depending on the bulk amount of sulfur, one or more sulfide liquids. The pressure, temperature and chemical composition of the system set the geochemical behaviour of the chemical elements, which partition into the different reservoirs according to their affinities: lithophile ("rock-loving") elements concentrate in the silicate portion of the planet; siderophile ("metal-loving") and chalcophile ("sulfide-loving") elements are mainly extracted to the core. The cooling and crystallization of the magma ocean lead to the formation of the mantle and the primitive crust. Subsequently, the internal energy of the young planet continues to dissipate, driving mantle melting and volcanic episodes that form a secondary crust. The *MESSENGER* spacecraft, which was launched by NASA in 2004 and spent four years orbiting the planet Mercury between 2011 and 2015 before its termination, has provided data on this secondary crust of Mercury.

Among the compositional data obtained by *MESSENGER*, the unusually high S and low FeO contents of the surface lavas has resulted in the idea that Mercury is a "reduced" planet, and that its formation and differentiation occurred under low oxygen fugacity (f_{O_2}) conditions (Zolotov et al. 2013). Such conditions are unique among the solar system's terrestrial planets and have induced a variety of features that, in combination, are peculiar to Mercury: a large and partially molten core (Hauck and Johnson 2019 this issue), explosive volcanism (Thomas and Rothery 2019 this issue), and exotic surface mineralogy (Namur and Charlier 2017). Moreover, because Mercury's extremely low f_{O_2} is comparable with that of enstatite meteorites, it is likely that Mercury's primitive building blocks formed in the solar nebula in similarly reducing environments.

MERCURY AND OTHER REDUCED SOLAR SYSTEM OBJECTS

How Do We Estimate the Oxygen Fugacity of Planetary Materials?

From a thermodynamic point of view, oxygen fugacity is equivalent to the equilibrium partial pressure (p) of oxygen in a given environment (e.g., the atmosphere, rocks, and so on). Air, which has a total pressure of 1.013 bar at sea level has a mole fraction of oxygen of 0.2095. This means that the f_{O_2} of air is 1.013 bar × 0.2095 = 0.212 bar (log f_{O_2} = –0.68), which results in highly oxidizing conditions. During the condensation of the first solids in the nebula, f_{O_2} was controlled by the partial pressure of O_2, which was itself imposed by the composition of the gas and, in particular, its high H/O ratio. This comes from the equilibrium:

$$H_2 + 0.5O_2 = H_2O \quad (1)$$

The equilibrium constant for reaction (1), K_w, is derived from thermodynamic measurements. At, for example 1,600 K, the logarithm of K_w is 5.185 (value from thermodynamic tables). This gives us:

$$\log K_w = 5.185 = \log \frac{p_{H_2O}}{p_{H_2} \cdot p_{O_2}^{0.5}} \quad (2)$$

If we make the usual assumption that the nebula pressure was 10^{-4} bar, then calculating all C as CO and the remaining O as H_2O yields an H_2O pressure of 5×10^{-8} bar. Given that the gas is > 99% H_2 means that p_{H_2} is almost exactly the same as the total pressure, i.e., 10^{-4} bar. Therefore,

$$\log p_{O_2} = 2p_{H_2O} - 2\log p_{H_2} - 10.37$$
$$\log p_{O_2} = 2(-7.3) - 2(-4) - 10.37 = -16.97 \quad (3)$$

with the result for p_{O_2} (or also f_{O_2}) in bar.

1 Centre de Recherches Pétrographiques et Géochimiques
Université de Lorraine, Nancy, France
E-mail: Camille.cartier@univ-lorraine.fr

2 Department of Earth Sciences
University of Oxford
Oxford, United Kingdom
E-mail: bernie.wood@earth.ox.ac.uk

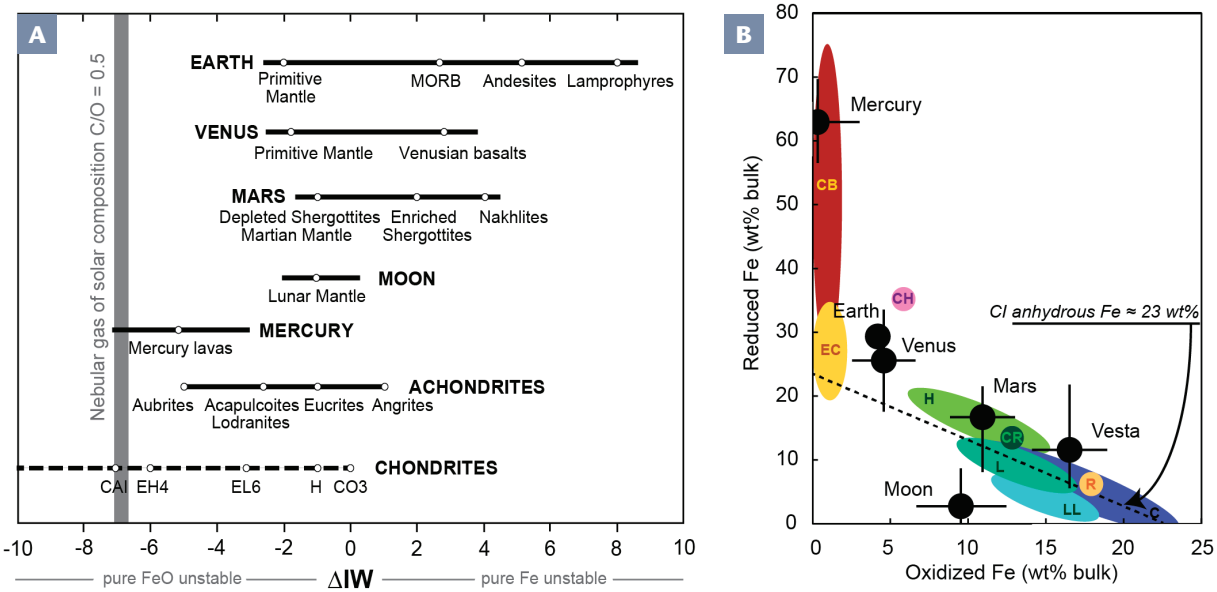

Figure 1 (**A**) Oxygen fugacities of various objects of the solar system, relative to iron–wüstite (IW) equilibrium, and compared with the f_{O_2} of a nebular gas of solar composition. Chondrite f_{O_2} range is represented by a dashed line to express that chondrites are highly unequilibrated objects. Abbreviations: CAI = calcium–aluminium inclusion; CO3 chondrite = carbonaceous Ornans-type chondrite, petrologic type 3; EH4 = high-enstatite chondrite, petrologic type 4; EL6 = low-enstatite chondrite, petrologic type 6; H chondrite = high-metal chondrite; MORB = mid-ocean ridge basalt. (**B**) Urey–Craig-type diagram showing Fe distribution in terrestrial planets and many varieties of chondrite (anhydrous bulk). "Oxidized Fe" occurs as or within silicates and oxides; "reduced Fe" occurs as or within metal and sulfides. Abbreviations: C = carbonaceous chondrite; CB = Bencubbin-type carbonaceous chondrite; CI = Ivuna-type carbonaceous chondrite; CH = high-metal carbonaceous chondrite; CR = Renazzo-type carbonaceous chondrite; EC = enstatite chondrite; H = high-metal chondrite; L = low total-Fe chondrite; LL = low total-Fe and low-metal chondrite; R = Rumuruti-type chondrite. Planetary and chondrite data calculated after Lodders and Fegley (1998) and Jarosewich (1990).

It is easier to conceptualize this result by considering elements such as Fe, which is more abundant than H_2 in terrestrial planets. If we react Fe metal with a sample of FeO (wüstite), then the f_{O_2} for the iron–wüstite equilibrium (IW) is defined by:

$$FeO = Fe + 0.5O_2 \quad (4)$$

At 1,600 K and 10^{-4} bar, the $\log(f_{O_2})$ or $\log(p_{O_2})$ for equilibrium (4) is –10.44, which means that the solar gas ($\log f_{O_2}$ = –16.97, from equation 3 above) is 6.5 $\log f_{O_2}$ units more reducing than the IW equilibrium (IW–6.5), which is shown in Figure 1A.

Given the high concentration of Fe in the solar system, f_{O_2} in planets is usually defined by the distribution of iron between its three common oxidation states: Fe^0, Fe^{2+} and Fe^{3+}. In the state of Fe^0, the element makes alloys, whereas the Fe^{2+} and Fe^{3+} states tend to form silicates and oxides. Thus, the oxidation state can be roughly translated into petrological terms and, at a planetary scale, into varying proportions of silicates, oxides, and metals. In the case of the Earth, the ratio of oxidized to reduced iron leads to an f_{O_2} about 2 log units below IW at the time of accretion; for Mars or Vesta, this ratio is about one log f_{O_2} unit more oxidized (Fig. 1).

Another way of estimating f_{O_2} consists of using oxybarometers. These are f_{O_2} proxies, experimentally calibrated and based on the change of valence state and/or the chemical behaviour of some elements, called "redox-sensitive elements", with f_{O_2}. For example, Ti, which occurs exclusively in the form of Ti^{4+} in terrestrial silicates, changes to Ti^{3+} under highly reducing conditions. Measuring the Ti^{3+}/Ti^{4+} ratio in a refractory calcium–aluminium-rich inclusion (CAI) embedded in a chondritic meteorite provides an estimate of 7 log units below IW (IW–7) for the conditions of condensation of these objects in the solar nebula (Grossman et al. 2008) (Fig. 1A).

Oxygen Fugacity on Mercury

A starting point for estimating the f_{O_2} of Mercury is to consider the distribution of Fe after segregation of the metallic Fe-rich core. The iron concentrations at the surface, as measured by *MESSENGER*, are 0.4 < Fe wt% < 2.7, with a mean content of 1.5 wt% (Weider et al. 2015). Assuming that all the iron is oxidized (i.e., in the form of FeO) and is representative of the planet bulk silicate, one can calculate an effective f_{O_2} in the range of 2.8 to 4.5 log units below IW. This makes Mercury the most reduced planet of the inner solar system (Fig. 1). When we investigate the details of Mercury's surface composition (Fig. 2), we find S contents up to 3.5%, which are values used by Namur et al. (2016a) as an alternative oxybarometer. Indeed, sulfur redox state and solubility in silicate melts is strongly dependent on oxygen fugacity (see discussion below). Using sulfur abundances in Mercury lavas, Namur et al. (2016a) estimated a mean f_{O_2} of IW–5.4.

The apparent mismatch between the f_{O_2} given by Fe and that given by S has often been considered a paradox, because at f_{O_2} < IW–4, experiments show that silicate melts do not contain more than 1 wt% FeO (Chabot et al. 2014; Malavergne et al. 2014) (Fig. 2). This paradox can be resolved by considering that, at Mercury's surface, Fe is mainly carried by sulfides (Ca–Mg sulfides containing a few wt% of Fe) (Fig. 2B) rather than silicates, something that has been suggested by spectral data. Such sulfides could have formed as an immiscible melt during core formation and be stored in the mantle.

The Redox Gradation Among Solar System Objects

It has been known for half a century that, in ordinary chondrites, the abundance of oxidized iron anticorrelates with the abundance of metal and the total iron amount (Urey and Craig 1953). This anticorrelation is illustrated in

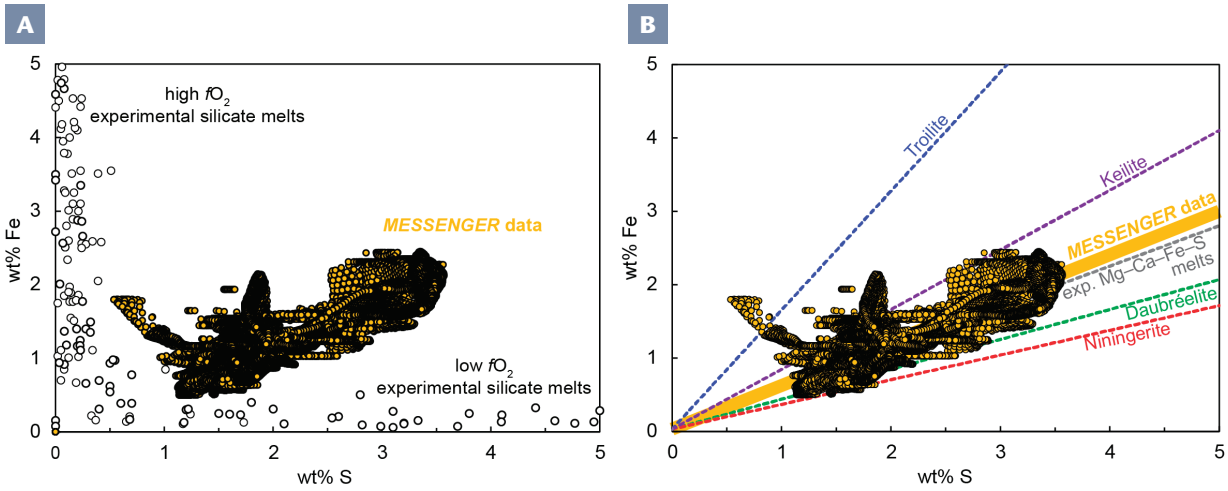

Figure 2 (**A**) Sulfur and iron contents measured at Mercury's surface (yellow dots) normalized to the mean Si surface content of 25 wt% and compared to experimental silicate melts compiled from the literature. This figure illustrates Mercury's "iron paradox" i.e., none of the experimental silicate melts, whatever the redox conditions, match Mercury's surface composition. (**B**) Sulfur and iron correlation at Mercury's surface matches the mean Fe/S ratio of Mg–Ca–Fe–S melts produced in highly reducing experiments and in some exotic sulfides found in enstatite meteorites, in particular daubréelite, niningerite and keilite. Therefore, the accumulation of different amounts of such a phase in Mercury's lavas is a possible explanation of Mercury's Fe paradox. Exp = experimental. Data from Weider et al. (2015).

a "Urey–Craig diagram", which plots oxidized iron contents versus reduced iron for terrestrial planets and for chondritic meteorites (Fig. 1B). Thus, most carbonaceous chondrites, which come from the outer part of the asteroid belt, are oxidized objects and their bulk iron content is similar to that of the nebula, as represented by CI (carbonaceous Ivuna-type) chondrites. In contrast, enstatite chondrites and bencubbinites are, together with Mercury, the most reduced objects. This gradation also correlates with water contents which seem, at first glance, to increase with heliocentric distance. The origin of these correlations is still debated, and various phenomena have been invoked: temperature-driven chemical fractionation during condensation of the nebular gas, magnetic and cosmic processes (such as photophoresis) and water-driven oxidation occurring during planetary migrations in the early solar system (Charlier and Namur 2019 this issue). The solar system's chemical gradation indicates that planetary accretion close to the Sun would probably produce a Mercury-like object. The high core/silicate ratio of Mercury may, therefore, simply reflect the environment of formation rather than, as has been suggested, mantle that has been lost by a giant impact. Further, the high core/silicate ratio also suggests that reduced meteorites, bencubbinites, enstatite chondrites, and enstatite achondrites (aubrites) may have formed in a similar nebular environment and under very low oxygen fugacities.

It is worth noting that Cr and Ti stable isotope compositions of meteorites and planets contradict the idea of a continuous chemical gradation in the solar system and show, on the contrary, a dichotomy (Warren et al. 2011). Interpreting the available data for these two stable isotopes suggests that the planetary objects of our solar system would be affiliated to two distinct reservoirs in the accretion disc: (1) an inner reservoir that would have given birth to the terrestrial planets and the ordinary and enstatite chondrites; (2) an outer reservoir, located beyond Jupiter's orbit, that would have given birth to carbonaceous chondrites, including the metal-rich bencubbinites.

Enstatite Meteorites: Mercury's Building Blocks?

Because of their apparent redox state, enstatite chondrites and bencubbin-like chondrites (CB chondrites) have historically been considered as possible building blocks for Mercury. In the following, we describe briefly these two groups of meteorites and show that neither of them match the bulk composition of Mercury. More generally, the idea that chondrites are planetary building blocks is challenged by the chemical and isotopic mismatches. The chondrites are better used to highlight special features of planets and assign them to particular conditions in the accretion disc. In addition, isotopic arguments seem to rule out the possibility of a genetic link between bencubbinites and Mercury (Warren et al. 2011). However, it is important to study these meteorites because they are the only ones to match Mercury's bulk iron content.

Enstatite Meteorites

Enstatite chondrites are dry and reduced meteorites which may be linked to M-type asteroids [those made dominantly Fe(Ni) metal] located in the innermost asteroid belt. Unlike other chondrites, which mainly contain olivine, their major silicate phase is near-pure end-member orthopyroxene (FeO < 1 wt%). They also contain large amounts (~13–28 vol%) of Fe(Ni) metal and this metal contains several wt% silicon. The combination of low FeO and Si-bearing metal indicates that enstatite chondrites formed in a very reduced nebular environment (see discussion below). Another remarkable feature of enstatite chondrites is the occurrence of a wide variety of unusual sulfides: mainly Ti–Cr-bearing troilite (FeS), oldhamite ((Ca,Mg)S), niningerite ((Mg,Fe,Mn)S) (Fig. 3) and other sulfides formed by cations that are usually lithophile (such as djerfisherite $K_6Na(Fe,Cu,Ni)_{25}S_{26}Cl$). The sulfides in enstatite chondrites also contain trace nitrides and carbides: the stabilities of such compounds also require extremely low f_{O_2} (Keil 2010), even more reducing than the solar gas (Fig. 1).

Aubrites are enstatite achondrites which share most of the special features of enstatite chondrites. They are mainly composed of FeO-free enstatite, minor albitic plagioclase, nearly FeO-free diopside and forsterite, and accessory exotic sulfides. As in enstatite chondrites, the sulfides in aubrites are formed by cations that are usually lithophile

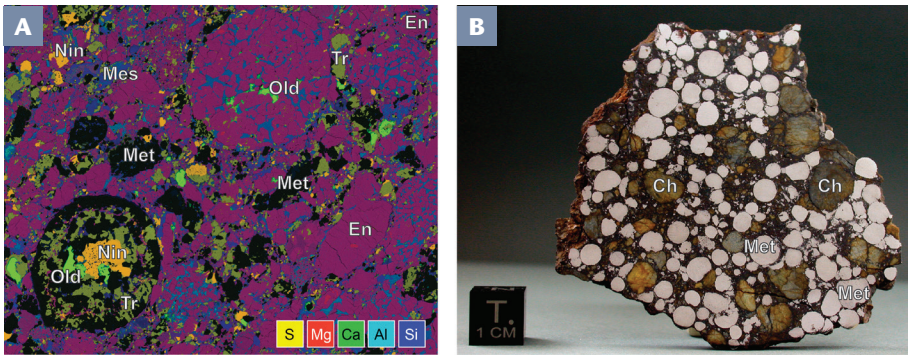

Figure 3 (**A**) Scanning electron microscope chemical map of an enstatite chondrite. The mineralogy of these meteorites is similar to the putative mineralogy of Mercury's mantle. Map courtesy L. Piani, Hokkaidō University, Japan. (**B**) Photograph of a bencubbin-like chondrite. These meteorites are the only ones to share Mercury's iron bulk abundance. Abbreviations: Ch = chondrule; En = enstatite; Mes = glassy mesostasis; Met = metal; Nin = niningerite; Old = oldhamite; Tr = troilite. Image credit S. Kamabch.

(Ca, Mg), and the trace iron-metal blebs contain significant amounts of Si (Keil 2010). At the moment, aubrites are the best analogue rocks of the surface of Mercury. Should any meteorites arrive from Mercury, they would almost certainly be classified as an aubrite. Petrology experiments show that partial melting of enstatite chondrites produce melts that, in terms of major elements, are similar to aubrites and to Mercury's surface composition (McCoy et al. 1999). This is principally due to their high S contents (3–5 wt%) and the virtual absence of FeO from their silicate. Enstatite chondrites cannot, however, be the major building blocks of Mercury because their bulk Fe content is too low (20–35 wt%) compared to that of Mercury (60–70 wt% Fe).

Bencubbinite (CB) Chondrites

Bencubbinites are a rare group of carbonaceous chondrites. As with other chondrites, they are aggregations of more or less spherical silicate and metal clasts, but they are distinguished by their extremely high modal abundance of Fe-rich metal (40–75 wt%) (Figs. 1 and 3). Trace siderophile element abundances and distribution among metal blebs suggest a mixed origin: part of the metal likely condensed from a nebular gas, whereas the rest probably came from the vaporization of planetesimal cores during violent impacts (Lauretta et al. 2009). However, although much richer in metal than enstatite chondrites, bencubbinites probably formed under less-reducing conditions, given the slightly higher FeO contents (≤ 3.5 wt%) of their silicates and more variable Si contents of their metals. Unlike enstatite chondrites, CB chondrites are highly depleted in moderately volatile lithophile elements (Lauretta et al. 2009). This results in CB chondrites being low in volatile sulfur: they contain few sulfide minerals, though principally Cr-bearing troilite. Thus, given their low-sulfur chemistry, they cannot be the source of the high-sulfur content of Mercury.

THE BEHAVIOUR OF ELEMENTS UNDER STRONGLY REDUCING CONDITIONS

There have been a number of studies aimed at understanding the behaviour of elements under the strongly reducing conditions of early Mercury (e.g., Kilburn and Wood 1997; Chabot et al. 2014; Namur et al. 2016a). Experimentally, conditions of IW–3 or lower can be reproduced with the use of a strong reducing agent, such as metallic Si which is mixed with the starting material prior to an experiment (Fig. 4). Metallic elements can undergo oxidation–reduction reactions analogous to reaction (4), which is the Fe–FeO equilibrium, that are mainly controlled by f_{O_2}. Let us consider the typically lithophile element silicon:

$$SiO_{2\ (silicate)} = Si_{\ (metal)} + O_{2(gas)} \quad (5)$$

As f_{O_2} is reduced, the reaction is "pulled" to the right, which tends to stabilize the metal at the expense of the oxide dissolved in the silicate. In this metal–silicate equilibrium, the geochemical behaviour of Si is quantified by its partition coefficient D_{Si}, defined as follows:

$$D_{Si} = \frac{[Si]_{metal}}{[Si]_{silicate}} \quad (6)$$

Thus, as can be seen in Figure 5B, Si becomes increasingly siderophile as f_{O_2} is reduced. At the conditions of Mercury differentiation, we therefore expect that a substantial amount of Si is incorporated in the core-forming alloys.

The opposite effect is observed for sulfur, which partitions less strongly into the metal with decreasing f_{O_2} and changes its behaviour from siderophile to lithophile under IW–5 (Fig. 5A). This can be understood in terms of the following equilibrium:

$$Fe_{(metal)} + S^{2-}{}_{(silicate)} + 0.5O_{2(gas)} = FeS_{(metal)} + O^{2-}{}_{(silicate)} \quad (7)$$

At high f_{O_2}, sulfur resides as FeS in the metal. As f_{O_2} is decreased, the reaction is pulled to the left, causing the S to enter the silicate melt as a sulfide species, resulting in S^{2-} replacing O^{2-} in the silicate framework. The metal then becomes S-poor (Kilburn and Wood 1997). Thus, the solubility of sulfur in silicate melts dramatically increases from <1 wt% S at IW–2 to >10 wt% S at IW–8 (Namur et al. 2016a). Under the redox conditions of Mercury, lavas will then contain several wt% sulfur.

At last, under strongly reducing conditions, many nominally lithophile elements, including uranium, partition strongly into the sulfide (Wohlers and Wood 2015). The reason for this can be understood in terms of the exchange of U and Fe between silicate and sulfide:

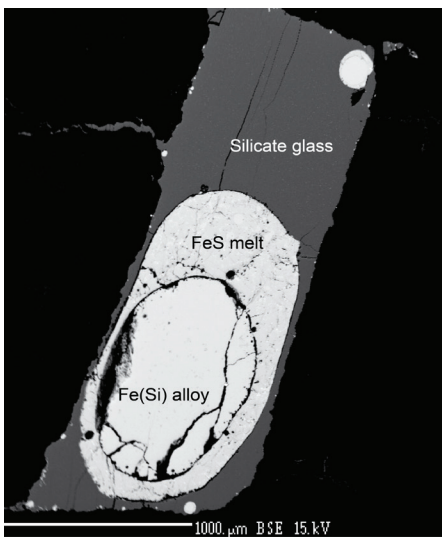

Figure 4 Backscattered electron image of an experimental charge. The experiment was performed by Namur et al. (2016a) at 5 GPa, 1,800 °C and at a fo_2 of IW–5.5 in order to simulate Mercury magma ocean conditions. Image courtesy O. Namur.

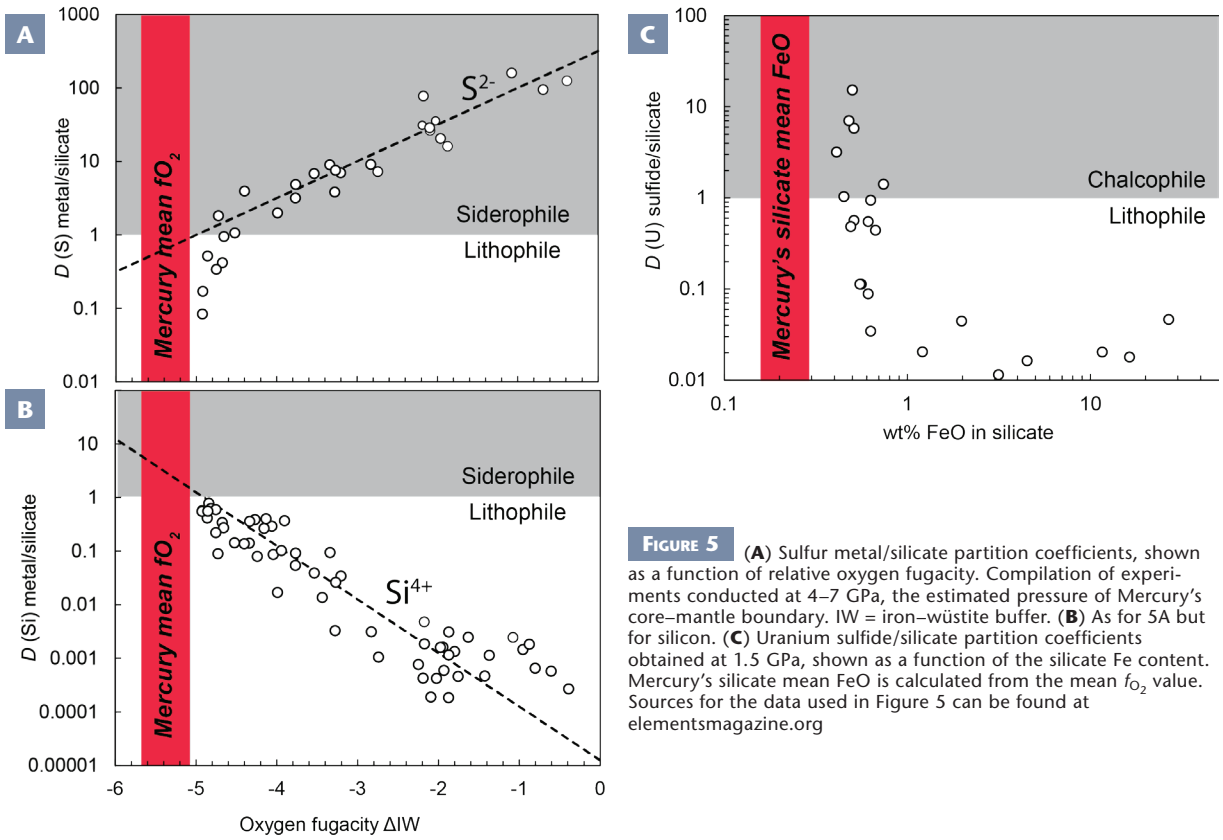

Figure 5 (**A**) Sulfur metal/silicate partition coefficients, shown as a function of relative oxygen fugacity. Compilation of experiments conducted at 4–7 GPa, the estimated pressure of Mercury's core–mantle boundary. IW = iron–wüstite buffer. (**B**) As for 5A but for silicon. (**C**) Uranium sulfide/silicate partition coefficients obtained at 1.5 GPa, shown as a function of the silicate Fe content. Mercury's silicate mean FeO is calculated from the mean f_{O_2} value. Sources for the data used in Figure 5 can be found at elementsmagazine.org

$$UO_{2(silicate)} + 2FeS_{(sulfide)} = 2FeO_{(silicate)} + US_{2(sulfide)} \quad (8)$$

By lowering the FeO content of the silicate, i.e., decreasing the f_{O_2}, we "pull" the equilibrium to the right, forcing U into the sulfide and increasing D_U (the partition coefficient of U between sulphide and silicate). As can be seen in Figure 5C, at the silicate melt compositions appropriate for Mercury (< 0.5 wt% FeO), U behaves as a chalcophile, with $D_U > 10$. This leads to the possibility of concentrating U in a potential sulfide layer which would provide a radioactive heat source at the top of the core.

MAKING MERCURY UNDER REDUCING CONDITIONS

Condensation–Accretion

The first stage of making Mercury involves condensation of a solar gas. During this process, lithophile elements, such as Ca and Mg, should condense into silicates while siderophile elements, such as Fe and Ni, should (according to thermodynamic calculations) condense into a metal alloy (Lodders 2003). During further cooling, sulfur reacts with the Fe to produce FeS, and many volatile chalcophile elements (e.g., Ag, Pb …) should enter this sulfide phase. As discussed above, the solar gas is quite reducing. Chemical reactions under such conditions explain the mineralogy of most chondrites, but not that of the more reduced meteorites, such as enstatite chondrites. The latter are notable for containing exotic sulfides and trace carbides and nitrides, which should not be produced from a gas of solar composition. One way of generating a stable assemblage of these compounds from a cooling solar-like gas is to enrich it in graphitic dust. Raising the C/O ratio increases the CO abundance, reduces the concentration of H_2O, raises H_2/H_2O, and lowers the f_{O_2} (Ebel and Alexander 2011). Given their reduced mineral assemblages, enstatite chondrites and the precursors of Mercury probably formed, at least in part, from primitive solids that condensed under such chemical conditions. A hot and highly reducing nebular environment plausibly existed close to the young Sun in a portion of the accretion disk enriched in C-bearing dust. The condensation of refractory sulfides of Ca and Mg – but also of K, Na and Cl (Ebel and Sack 2013) – in such a nebular environment would also have led to the apparent enrichment of Mercury in elements (such as S, Na, K, Cl) that are normally regarded as volatile and, hence, expected to be depleted in the inner solar system. In the same way, the presence of carbon in the form of refractory graphite would have contributed to the bulk "volatile" budget of the planet.

Core Formation

The segregation of a metal core is likely to have continued throughout Mercury's accretion during multiple magma-ocean episodes (Fig. 6). At an estimated f_{O_2} around 5.4 log units below IW, almost all Fe is present as metal (Fe^0) and forms alloys with significant amounts of Si, because the metal/silicate partition coefficient of Si is close to 1 (Fig. 5). Assuming that Mercury's silicate shell is peridotitic in Si content (~20 wt%), the equilibrium metal should, therefore, contain about 20% Si. This estimate is consistent with geophysical models that predict about 15 wt% Si in Mercury's core (Margot et al. 2018). Silica lowers the core melting temperature, thus, the expected Si core content could explain why a large portion of Mercury's core is still molten and is still generating a magnetic field (Knibbe and van Westrenen 2018).

Under these conditions, there is a large miscibility gap in the Fe–Si–S liquid system (Morard and Katsura 2010), which means that any excess metallic FeS forms a separate phase (Fig. 4). These conditions are so reducing, however, that S also behaves as a lithophile element that dissolves in the magma ocean in the form of S^{2-} (Fig. 5A) and is bound mainly to Ca, Mg and the little remaining Fe (Namur et al. 2016a). Assuming that, during core segregation, the silicate

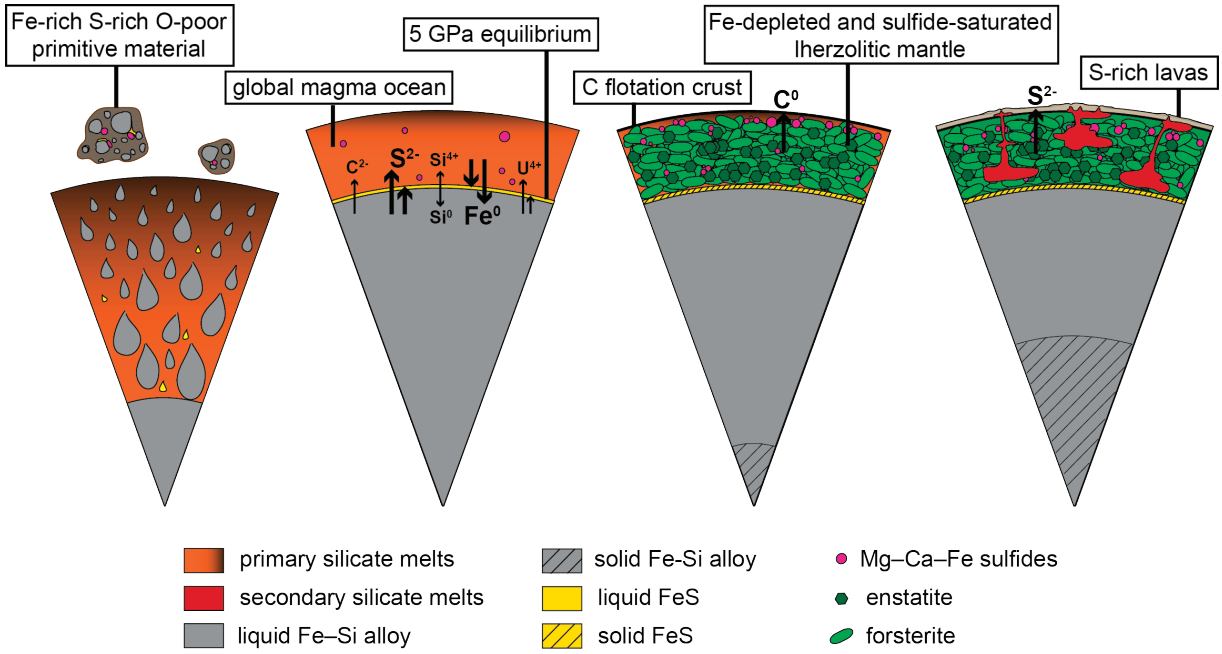

Figure 6 Summary sketch showing the four main steps of Mercury's formation: accretion, core formation, magma ocean crystallization and secondary volcanism. At each stage, very low oxygen fugacities influenced the behaviour of elements. Arrows schematize element partitioning, with big arrows for contrasted behaviour (partition coefficients >> or << 1) and small arrows for more equitable partitioning (partition coefficients ≤ or ≥ 1).

was sulfide-saturated, this would then lead to 7–11 wt% S in the silicate mantle (Namur al. 2016a). Immiscibility between Fe–Si liquids and FeS would result in an intermediate-density layer of sulfide above the metallic core. The thickness of this putative sulfide layer (Fig. 6) would depend on the total S content of the planet. This is difficult to quantify because the abundance of sulfur is extremely variable between the different chondrite classes. Because enstatite chondrites show the highest sulfur contents (5.8 wt% for high-iron meteorites), they can be used as an upper limit. Assuming sulfide saturation of the mantle and this maximum plausible S content, an FeS layer of about 90 km thickness can be calculated. The formation of an FeS layer during Mercury's differentiation is of particular importance because it would have trapped significant amounts of U, which is the main radioactive heat-producing element of planetary interiors (Fig. 5C) (Wohlers and Wood 2015). However, as the sulfide would only be 90 km thick at its maximum, the main uranium budget (more than 85%) would remain in the silicate magma ocean after core formation. It should also be noted that, during core formation, small quantities of an additional immiscible Mg–Ca–Fe sulfide melt (such a melt having been found in some extremely reducing experiments) could have stayed in the magma ocean. Such a phase could explain how Mercury is so reduced but still store little iron in its silicate (Malavergne et al. 2014) (Fig. 2). Finally, carbon, in a manner analogous to sulfur, likely adopts lithophile behaviour under highly reducing conditions and concentrates in the silicate portion of the planet at the expense of the core. Although experimental data relevant to Mercurian conditions for C are still scarce, a recent study shows that reducing conditions tend to exclude C from the metal phase (Li et al. 2017).

Magma Ocean Crystallization

As the planet cooled and the silicate crystallized, we anticipate that there formed a crystalline assemblage dominated by forsterite and enstatite, with lesser amounts of clinopyroxene and minor amounts of CaS, MgS and FeS. Experiments conducted on analogues of Mercury's surface lavas, allied to chemical modelling, confirm that the liquids were produced by partial melting of lherzolitic mantle under highly reducing conditions (Namur et al. 2016b). Due to the crystallization of mafic minerals, the magma ocean would have been concentrated in incompatible carbon to finally reach graphite saturation (Li et al. 2017) and precipitation. This graphite would be buoyant and rise through the melt column to form a primary flotation crust (Fig. 6). The possible role of graphite flotation and the formation of an early crust are consistent with the detection of endogenic graphite at Mercury's surface (Peplowski et al. 2016).

The Later Stages of Secondary Volcanism and Surface Processes

Between 4.2 Ga and 3.7 Ga, Mercury's mantle underwent repeated melting events that contributed to the strong secular cooling of the planet (Namur al. 2016b) and to the formation of its secondary volcanic crust. Although effusive volcanism shaped much of Mercury's surface, a few pyroclastic deposits and volcanic vents show that explosive volcanism also existed (Thomas and Rothery 2019 this issue). Explosive eruptions are driven by the exsolution of volatile species from the liquid phase during magma decompression. On Earth, the main volatile species involved in volcanism are CO_2, H_2O and SO_2. On Mercury, the very low f_{O_2} would, depending on H content, tend to favour the stability of CO, COS, and S_2 gases (Zolotov 2011). During Mercury's mantle melting, the pressure–temperature–f_{O_2} conditions allowed 1–4 wt% sulfur to dissolve in the silicate liquids in the form of sulfide complexes (Namur et al. 2016a). These partial melts ascended through the mantle and eventually came into contact with the putative primary graphite-rich crust, possibly entraining graphite crystals during their continued ascent (McCubbin et al. 2017). As these partial melts ascended through the crust, primary melts also came into contact with crustal silicates. The assimilation of oxides from crustal rocks into shallow magma chambers would have led to the partial oxidation of the sulfide complexes in the silicate melt, producing

volcanic S_2 (Zolotov 2011). Additionally, some silicate melt oxides would have been reduced to metals by the graphite (during a reaction similar to the "smelting" process used in metallurgy), producing a substantial volume of CO (McCubbin et al. 2017). Once the lavas erupted and the volatiles liberated, additional graphite might also have reacted with surface material and reduced some SiO_2 to metallic Si. This phenomenon could account, together with space weathering, for the underabundance of oxygen relative to cation-forming elements at the surface of Mercury (McCubbin et al. 2017). Finally, depending on cooling rates at the planetary surface, the melt could have quenched as a glass or could have crystallized minerals dominated by plagioclase, diopside, forsterite, enstatite, a SiO_2 phase, and various sulfides (mainly CaS, MgS and FeS) (Namur and Charlier 2017). Such a surface mineralogy is an additional feature that makes Mercury unique among the terrestrial planets.

SUMMARY

Mercury displays unique characteristics that make it an end-member of our solar system (Charlier and Namur 2019 this issue). These exotic features – an extremely large and silicon-rich core, a graphitic primary crust, and a secondary crust made of S-rich/FeO-poor lavas – are the consequence of Mercury differentiating under highly reducing conditions. The intrinsic low f_{O_2} of Mercury's building materials is itself inherited from particular nebular conditions. The planet probably accreted in a portion of the nebular disk that was enriched in graphitic dust and that was very close to the Sun.

REFERENCES

Charlier B, Namur O (2019) Origin and differentiation of planet Mercury. Elements 15: 9-14

Chabot NL, Wollack EA, Klima RL, Minitti ME (2014) Experimental constraints on Mercury's core composition. Earth and Planetary Science Letters 390: 199-208

Ebel DS, Alexander CMO'D (2011) Equilibrium condensation from chondritic porous IDP enriched vapor: implications for Mercury and enstatite chondrite origins. Planetary and Space Science 59: 1888-1894

Ebel DS, Sack RO (2013) Djerfisherite: nebular source of refractory potassium. Contributions to Mineralogy and Petrology 166: 923-934

Grossman L, Beckett JR, Fedkin AV, Simon SB, Ciesla FJ (2008) Redox conditions in the solar nebula: observational, experimental, and theoretical constraints. Reviews in Mineralogy and Geochemistry 68: 93-140

Hauck SA II, Johnson CL (2019) Mercury: inside the iron planet. Elements 15: 21-26

Jarosewich E (1990) Chemical analyses of meteorites: a compilation of stony and iron meteorite analyses. Meteoritics and Planetary Science 25: 323-337

Keil K (2010) Enstatite achondrite meteorites (aubrites) and the histories of their asteroidal parent bodies. Chemie der Erde - Geochemistry 70: 295-317

Kilburn MR, Wood BJ (1997) Metal–silicate partitioning and the incompatibility of S and Si during core formation. Earth and Planetary Science Letters 152: 139-148

Knibbe JS, van Westrenen W (2018) The thermal evolution of Mercury's Fe–Si core. Earth and Planetary Science Letters 482: 147-159

Lauretta DS and 8 coauthors (2009) The Fountain Hills unique CB chondrite: insights into thermal processes on the CB parent body. Meteoritics and Planetary Science 44: 823-838

Li Y, Dasgupta R, Tsuno K (2017) Carbon contents in reduced basalts at graphite saturation: implications for the degassing of Mars, Mercury, and the Moon. Journal of Geophysical Research: Planets 122: 1300-1320

Lodders K (2003) Solar system abundances and condensation temperatures of the elements. Astrophysical Journal 591: 1220-1247

Lodders K, Fegley B Jr (1998) The Planetary Scientist's Companion. Oxford University Press, 400 pp

Malavergne V and 11 coauthors (2014) How Mercury can be the most reduced terrestrial planet and still store iron in its mantle. Earth and Planetary Science Letters 394: 186-197

Margot J-L, Hauck SA II, Mazarico E, Padovan S, Peale SJ (2018) Mercury's internal structure. In: Solomon SC, Nittler LR, Anderson BJ (eds) Mercury: The View after *MESSENGER*. Cambridge University Press, Cambridge, pp 85-113

McCoy TJ, Dickinson TL, Lofgren GE (1999) Partial melting of the Indarch (EH4) meteorite: a textural, chemical, and phase relations view of melting and melt migration. Meteoritics and Planetary Science 34: 735-746

McCubbin FM and 9 coauthors (2017) A low O/Si ratio on the surface of Mercury: evidence for silicon smelting? Journal of Geophysical Research: Planets 122: 2053-2076

Morard G, Katsura T (2010) Pressure–temperature cartography of Fe–S–Si immiscible system. Geochimica et Cosmochimica Acta 74: 3659-3667

Namur O, Charlier B (2017) Silicate mineralogy at the surface of Mercury. Nature Geoscience 10: 9-13

Namur O, Charlier B, Holtz F, Cartier C, McCammon C (2016a) Sulfur solubility in reduced mafic silicate melts: implications for the speciation and distribution of sulfur on Mercury. Earth and Planetary Science Letters 448: 102-114

Namur O and 5 coauthors (2016b) Melting processes and mantle sources of lavas on Mercury. Earth and Planetary Science Letters 439: 117-128

Peplowski PN and 9 coauthors (2016) Remote sensing evidence for an ancient carbon-bearing crust on Mercury. Nature Geoscience 9: 273-276

Thomas RJ, Rothery DA (2019) Volcanism on Mercury. Elements 15: 27-32

Urey HC, Craig H (1953) The composition of the stone meteorites and the origin of the meteorites. Geochimica et Cosmochimica Acta 4: 36-82

Warren PH (2011) Stable-isotopic anomalies and the accretionary assemblage of the Earth and Mars: a subordinate role for carbonaceous chondrites. Earth and Planetary Science Letters 311: 93-100

Weider SZ and 10 coauthors (2015) Evidence for geochemical terranes on Mercury: global mapping of major elements with MESSENGER's X-Ray Spectrometer. Earth and Planetary Science Letters 416: 109-120

Wohlers A, Wood BJ (2015) A Mercury-like component of early Earth yields uranium in the core and high mantle ^{142}Nd. Nature 520: 337-340

Zolotov M (2011) On the chemistry of mantle and magmatic volatiles on Mercury. Icarus 212: 24-41

Zolotov MY and 5 coauthors (2013) The redox state, FeO content, and origin of sulfur-rich magmas on Mercury. Journal of Geophysical Research: Planets 118: 138-146